Magnus Forces on Spinning Supersonic Cones – Part I: The Boundary Layer

H. A. Dwyer*
University of California at Davis, Davis, Calif.

and

B. R. Sanders†
Sandia Laboratories, Livermore, Calif.

A detailed investigation of the laminar boundary-layer flow over a spinning right-circular cone at small angle of attack has shown that there are at least four significant forces contributing to the Magnus force on the cone. In order to calculate these forces, a novel numerical method has been developed which can calculate these small forces over a wide range of flow parameters. The flow conditions have a large influence on the relative magnitude of the Magnus force components, and there can be significant cancelling of the various components.

Introduction

THIS investigation is an attempt to develop a method of calculating the force due to spin (Magnus force) on a right-circular cone at small angle of attack in supersonic flow. Although the force usually is very small, its nature is quite complicated; therefore in this investigation the flow geometry and gas properties have been kept simple. Thus, the paper will be limited to laminar flow of a perfect gas and will focus on identifying the important mechanisms generating boundary-layer forces. However, in order to exhibit clearly the various components of the Magnus force, a considerable variation in Mach number, wall temperature, angle of attack, and spin rates will be employed. It also will be shown that conventional boundary-layer theory is capable of treating this problem in the important case of small angle of attack.

During the past 20 years, some important investigations have contributed to our knowledge of the Magnus force on a spinning body at angle of attack. A valuable solution was developed by Sedney,[1] for conditions similar to those described in the present paper. Sedney's solution consisted of a regular perturbation expansion and series solution of the boundary-layer equations based on spin rate and angle of attack. Because of the many parameters in the problem and the complexity imposed by the many terms in the series, this method can be used only to calculate the boundary-layer flow for small spin rates and angle of attack. Also, Sedney used slender body theory to calculate the displacement-thickness contribution of the Magnus force, an approach that introduces further restriction and approximation into the method. Therefore, Sedney's solution does not have enough flexibility to be used over a wide range of flow parameters and cannot be extended readily to turbulent flow and more general body shapes.

A more recent theory, developed by Vaughn and Reis,[2] has been applied both to laminar and turbulent flow. However, the theory applies many unproved assumptions on both the primary and crossflow velocity profiles and uses two-dimensional correlations to estimate the influence of heat transfer. Slender-body theory also is used to calculate the displacement-thickness contribution to the Magnus force. It seems clear at this time that the methods used in Ref. 2 must first be checked before they can be used with confidence.

An excellent recent investigation on Magnus forces has been reported by Lin and Rubin.[3] The main thrust of this paper is to calculate a leading-edge interaction region at hypersonic speeds and to apply boundary-region techniques on spinning cones. However, the study did not cover completely the various components of the Magnus force; and again, slender body theory was employed for the displacement-thickness contribution.

Since the present paper is concerned mainly with numerical methods, a thorough discussion of experimental investigations will not be carried out. Some additional experimental work is cited in Refs. 1-3, and a series of excellent investigations has been carried out recently by Sturek,[4,5] who discusses in detail the influence of transition from laminar to turbulent flow on the Magnus force. A comparison of the present results with those of other studies is given in Part II.

In this paper, numerical solutions of the laminar boundary-layer flow will be presented for a wide range of flow parameters. From these solutions it will be shown that there are four significant boundary-layer forces, which contribute to the Magnus force. These forces are: 1) displacement-thickness interactions; 2) centrifugal pressure gradients; 3) crossflow shear, and 4) primary-flow shear. Depending on the flow conditions, the various forces can vary considerably; however, the primary-flow shear contribution is always much smaller than the other effects. All of the force contributions except that due to displacement thickness are presented in Part I of this paper, and an exact method of solution for the force due to displacement thickness has been developed in

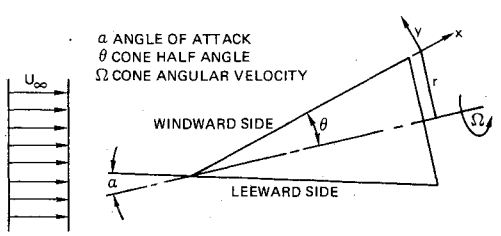

Fig. 1 Cone geometry.

Presented as Paper 75-183 at the AIAA 13th Aerospace Sciences Meeting, Pasadena, Calif., January 20-22, 1975; received May 23, 1975; revision received October 20, 1975. This work was partially supported by the U.S. Energy Research and Development Administration. Contract Number AT-(29-1)-789. The authors would like to thank W. Sturek, R. Sedney, W. Kitchens, and F. Blottner for the many insights they have given on a very long and tedious journey to the solution of this problem.

Index categories: Boundary Layers and Convective Heat Transfer-Laminar; Supersonic and Hypersonic Flow.

*Professor, Dept. of Mechanical Engineering. Member AIAA.

†Member of the Technical Staff, Combustion Research Div. Member AIAA.

Part II. Also, the methods developed in the paper can be extended to the important cases of turbulent flow and ogive bodies.

Basic Equations

The basic flow geometry and coordinate systems to be employed for the flow over a spinning right-circular cone are shown in Fig. 1. With spin, the boundary-layer flow is completely three-dimensional and a similarity variable along the cone surface no longer can be defined. In terms of the coordinates shown in Fig. 1, the boundary-layer approximation yields the following equations:

$$\frac{\partial}{\partial x}(\rho r u) + \frac{\partial}{\partial y}(\rho r v) + \frac{1}{r}\frac{\partial}{\partial \phi}(\rho r w) = 0 \qquad \text{(continuity)}$$

$$\rho u\frac{\partial u}{\partial x} + \rho v\frac{\partial u}{\partial y} + \frac{\rho w}{r}\frac{\partial u}{\partial \phi} - \frac{\rho r' w^2}{r} = +\frac{\partial}{\partial y}\left(\mu\frac{\partial u}{\partial y}\right) \qquad (x\text{-momentum})$$

$$\rho u\frac{\partial w}{\partial x} + \rho v\frac{\partial w}{\partial} + \frac{\rho w}{r}\frac{\partial w}{\partial \phi} + \frac{\rho r' uw}{r} = -\frac{1}{r}\frac{\partial p}{\partial \phi} + \frac{\partial}{\partial y}\left(\mu\frac{\partial w}{\partial y}\right) \qquad (\phi\text{-momentum})$$

$$\rho C_p u\frac{\partial T}{\partial x} + v\frac{\partial T}{\partial y} + \frac{w}{r}\frac{\partial T}{\partial \phi} = u\frac{\partial p}{\partial x} + \frac{w}{r}\frac{\partial p}{\partial \phi} + \mu\left[\left(\frac{\partial u}{\partial y}\right)^2 + \left(\frac{\partial w}{\partial y}\right)^2\right] + \frac{\partial}{\partial y}\left(k\frac{\partial T}{\partial y}\right) \qquad \text{(energy)}$$

where u, v, and w are the velocities on the x, y, and ϕ (angular) directions, respectively, ρ is density, T is temperature, μ is viscosity, k is thermal conductivity; r' is dr/dx; p is pressure, and C_p is specific heat at constant pressure. As in two-dimensional problems, the physical coordinate system is not an optimal one for carrying out numerical computations. In fact, at least an order-of-magnitude decrease in the number of computations can be achieved by working in a transformed coordinate system. A very good system to use for the present problem is the one developed by Moore[6] for another problem, which is

$$n = \int_0^y \frac{T_\infty}{T}\left(\frac{p_1}{p_\infty}\right)^{1/2}\left(\frac{3}{2}\frac{\rho_\infty u_\infty}{\mu_\infty x}\right)^{1/2} dy$$

$$\bar{x} = C^2 x^3/3$$

$$\phi = \phi$$

where all variables with subscript ∞ are reference variables (usually chosen on the windward side at the boundary-layer edge), C is equal to the sine of the cone half-angle, and subscript 1 is the local inviscid flow condition. The boundary-layer equations in terms of these variables become

$$\bar{x}\frac{\partial u}{\partial \bar{x}} - \frac{n}{6}\frac{\partial u}{\partial n} + \frac{\partial \bar{V}}{\partial n} + \frac{1}{3C}\frac{\partial w}{\partial \phi} - \frac{n}{6C}\frac{1}{p_1}\frac{\partial p_1}{\partial \phi}\frac{\partial w}{\partial n} = -\frac{u}{3} \qquad \text{(continuity)}$$

$$\bar{x}u\frac{\partial u}{\partial \bar{x}} + \mathcal{V}\frac{\partial u}{\partial n} + \frac{w}{3C}\frac{\partial u}{\partial \phi} - \frac{w^2}{3} = \frac{u_\infty}{2}\frac{\partial^2 u}{\partial n^2} \qquad (x\text{-momentum})$$

$$\bar{x}u\frac{\partial w}{\partial \bar{x}} + \mathcal{V}\frac{\partial w}{\partial n} + \frac{w}{3C}\frac{\partial w}{\partial \phi} + \frac{uw}{3} = \frac{u_\infty}{2}\frac{\partial^2 w}{\partial n^2} - \frac{1}{3C\rho}\frac{\partial p_1}{\partial \phi} \qquad (\phi\text{-momentum})$$

$$\bar{x}u\frac{\partial T}{\partial \bar{x}} + \mathcal{V}\frac{\partial T}{\partial n} + \frac{w}{3c}\frac{\partial T}{\partial \phi} = \frac{w}{3CC_p}\frac{1}{\rho}\frac{\partial p_1}{\partial s} + \frac{u_\infty}{2C_p}\left[\left(\frac{\partial u}{\partial n}\right)^2 + \left(\frac{\partial w}{\partial n}\right)^2\right] + \frac{u_\infty}{2Pr}\frac{\partial^2 T}{\partial \eta^2} \qquad \text{(energy)}$$

where

$$\mathcal{V} = \bar{V} - \frac{nu}{6} - \frac{n}{6C}\frac{w}{p_1}\frac{\partial p}{\partial \phi} \text{ and}$$

$$\bar{V} = \frac{\rho_\infty u_\infty}{2\mu_\infty}\left(\frac{p_\infty}{p_1}\right)^{1/2}\frac{\phi^{1/2}}{r}v$$

$$\phi = \bar{x}/\bar{l}^2 \qquad \bar{l}^2 = \rho_\infty u_\infty/2\mu_\infty$$

For the derivation of the preceding equations, the viscosity is assumed to be linear with temperature, the fluid an ideal gas, and the Prandtl number constant. Also, the flow variables u, w, and T have not been normalized because the inviscid flow changes very little, except for w_1, and because normalizing would have added many terms to the equations. In terms of the transformed coordinates, the boundary layer changes very slowly as compared with changes in physical coordinates; much larger steps can be taken in the numerical solution without convergence suffering.

The boundary conditions for the present problem will be very similar to those for a cone without spin. For the outer inviscid flow, the authors have used the solutions tabulated by Jones.[7] These agree very closely with the results obtained in Part II. At the surface, the velocities u and v are zero, while w increases linearly with x because of the spin. For all of the problems presented in this research, the wall temperature has been kept constant, but it has differed considerably from the adiabatic wall temperature.

Numerical Method

Over the past ten years, many numerical methods have been developed to solve the three-dimensional boundary-layer equations,[8-12] and they have yielded converged solutions to many problems. However, the spinning-cone problem presents a difficult challenge, since the surface flow caused by spin forms a streamline which is a circle. In principle, one cannot take a step in the x direction without violating the zone of influence,[13] but for finite step sizes Δx and Δy, the primary flow velocity u is nonzero, and a calculation can proceed without violating the zone of influence. The surface spin also causes the streamlines across the boundary layer to change in direction by more than 90°, and the crossflow changes sign. Since the sign of the velocity determines the direction in which convection occurs, any numerical method should reflect this change in sign if it is to model correctly the physical processes in the boundary layer. None of the numerical methods developed previously properly models the convection process; however, the present research uses a new method, which models convection more closely. The method, termed in Ref. 14 a "physically optimum" one, does respond to changes in the convection direction.

The basic finite-difference method is a variation of the implicit schemes, which have been used with great success in most of the three-dimensional methods mentioned previously. The scheme is set up so that the boundary-layer flow is calculated in planes from the cone tip. The first step is to

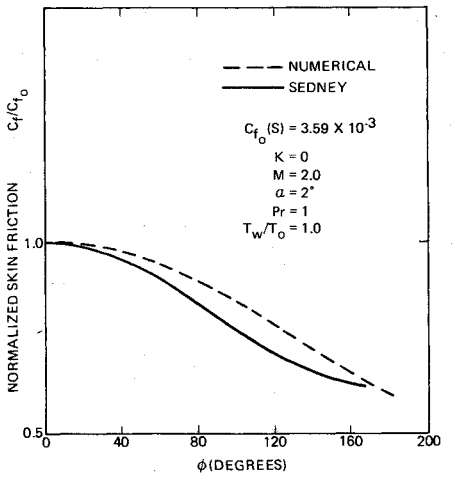

Fig. 2 Comparison with Sedney solution—no spin.

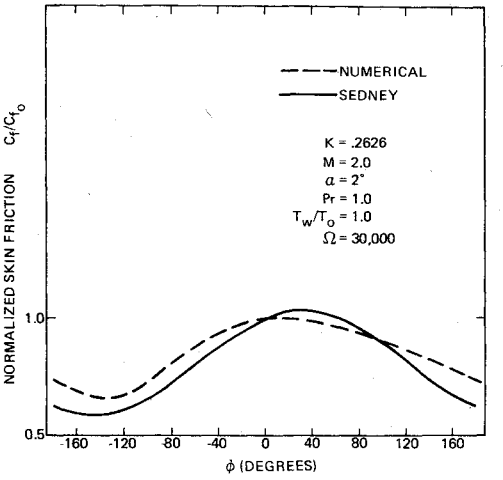

Fig. 3 Comparison with Sedney solution—spin.

calculate the flow at the cone tip. Actually, the flow is singular at that point, but in the transformed coordinate system the singularity is removed. The spin velocity at the tip is zero; therefore, the tip problem reduces to that of a nonspinning right-circular cone at angle of attack, and in order to solve this flow, the method developed by Dwyer and Sanders[14] was employed. With an initial plane of the boundary-layer flow known, the next plane is calculated in rows across the boundary layer. The scheme developed used implicit central differences for all n derivatives (boundary-layer coordinate) at the unknown grid station. For both the x and ϕ directions, backward differences always are applied. Since the crossflow w changes sign across the boundary layer in the spinning-cone problem, the grid points actually used to calculate a backward ϕ derivative will depend on the direction of the crossflow. The ϕ derivatives are evaluated explicitly in the previous plane. With this type of directional finite-difference scheme, the convection processes in the boundary layer in the x and ϕ directions are properly modeled physically. However, the overall accuracy of the method is first-order.

Because of the nonlinear nature of the boundary-layer equations, an exact stability analysis of the finite-difference scheme cannot be carried out. However, a linearized analysis can be accomplished, and such has been reported by Dwyer and Sanders.[14] The results of the analysis show that because of the explicit evaluation of the ϕ derivatives, there is a stability restriction on step size. To keep the method stable, the ratio of Δx to $r\Delta\phi$ must be chosen so that the zones of influence are not violated. Mathematically, this restriction implies that $\Delta x/r\Delta\phi \leq u/w$ for all points at which the boundary-layer calculation is performed. It should be mentioned, however, that if this condition is violated, the instability grows in a significantly slower manner than the one normally encountered by explicit techniques in two-dimensional boundary-layer problems. In fact, in the present investigation, the zone of influence has been violated grossly (step sizes 10 times larger than required), and useful results have been obtained which agree closely with the converged solutions that obey the zone of influence. One possible reason for this behavior could be the very small influence of spin on boundary-layer structure. In previous investigations, other three-dimensional boundary-layer problems[16] have been solved by violating the zone of influence and have agreed with exact solutions. A general rule cannot be formulated for violating the zone of influence; and if it is violated, the results must be checked by a solution that is exact or obeys the zone of influence.

Results

The first calculations to be presented are those that are designed to compare with the series solution of Sedney. The wall stress in the primary flow direction has been chosen as the comparison variable, since it is a derivative of the solution and is therefore more sensitive to convergence. Also, the primary-flow wall stress is the major contributor to forming the displacement thickness on the spinning cone. The results of the comparison for a nonspinning cone are shown in Fig. 2, where the skin-friction coefficient, normalized by its value at the windward line of symmetry, is given (note: these results are also those at the cone tip). At the windward line itself, the numerical solution and Sedney's agreed to within 1%; this result is to be expected since the same equations were solved. In order to obtain the equations for the cone tip, the limit is taken as $\bar{x} \to 0$, and at the windward line, the symmetry conditions must be applied.

As can be seen from Fig. 2, there is general agreement between the present numerical solutions for $M = 2.0$, $Pr = 1.0$, $\alpha = 2.0°$, $\theta = 10°$ and an adiabatic wall. The specific agreement, however, is not extremely good, the local value of shear disagreeing by as much as 15%. The reason for this disagreement is mainly the unavoidable fact that only a few terms can be calculated easily in the expansion. Sedney's solution has both an inviscid and a boundary-layer flow, which varies like $\sin\phi$; and investigations[14] on nonspinning cones have shown that this simple variation cannot describe the boundary-layer flow on the leeward side of the cone. It also should be mentioned that both solutions in Fig. 2 are converged to less than 0.1%.

Shown in Fig. 3 is another comparison of primary-flow wall shear, but for a cone spinning at 30,000 rpm. The spin parameter ($K = \Omega r/U_1$) has a rather large value of 0.2626, and spin has substantially altered the primary-flow skin friction. On the windward side ($\phi = 0$), the numerical solution agrees with Sedney's in predicting an almost negligible influence of spin at that location. On the leeward side, the perturbation expansion again predicts negligible influence of spin, and this result disagrees with the present numerical solutions. It must be concluded that the retarded boundary layer near the inviscid symmetry plane is responsive to spin, and this characteristic is important since the boundary layer thickens considerably in this region. In Fig. 3, the spin-induced crossflow is in the same direction as the inviscid crossflow for positive ϕ, and opposite to the inviscid crossflow for negative values of ϕ. For both the present and Sedney's solutions, the crossflow increases wall shear when it is positive (ϕ positive) and decreases wall shear when it is negative (ϕ negative). The minimum of wall shear moves substantially away from the leeward inviscid symmetry plane, and its location ($\phi = -135°$ for 1 ft down a 10° half-angle cone, $Re_\infty = 1.74 \cdot 10^6$) is predicated rather well by the expansion solution. It must be concluded, however, that the series solution does not have enough flexibility on the leeward side of the cone. Also, it should be mentioned again that both solutions are converged to within 0.1%.

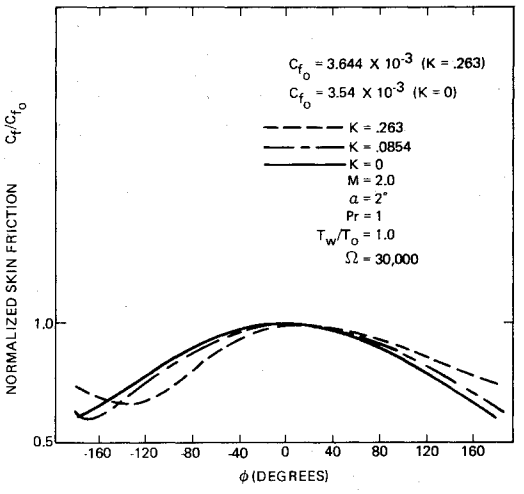

Fig. 4 Influence of spin on wall shear.

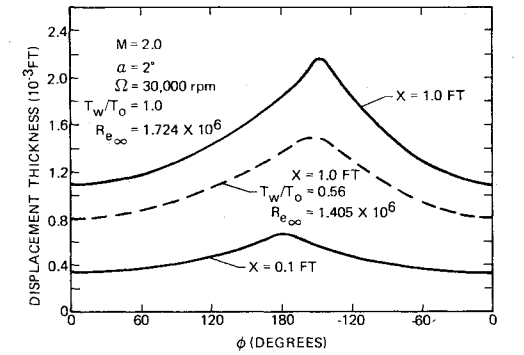

Fig. 5 Three-dimensional boundary-layer displacement thickness.

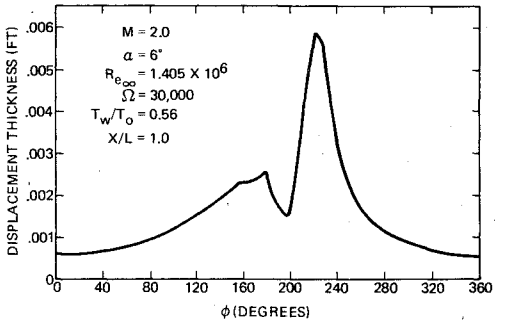

Fig. 6 Large angle of attack solution.

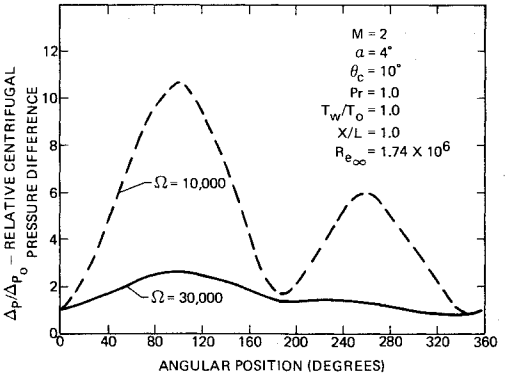

Fig. 7 Centrifugal pressure difference.

The influence of spin on primary-flow wall shear can be seen more explicitly in Fig. 4. Three values of spin rate have been chosen to illustrate the numerical solution. It is easily seen from this illustration how positive crossflow increases wall shear and negative crossflow decreases shear. At the leeward side, the wall shear increases in value with spin and the minimum shear location moves substantially away from the 180° location. Also, it can be concluded that spin slightly increases the value of minimum wall shear over the body. This effect could have some influence on transition; however three-dimensional transition is a very complicated subject, and suggestions must be made with caution. At the windward side ($\phi = 0°$) the wall shear increased by slightly less than 1%, even through the spin parameter was taken through a large variation.

The previous solutions have been obtained with a grid spacing that consisted of 60 points across the boundary layer ($0 \leqq n \leqq 6.0$) and 36 points around the body ($0 \leqq \phi \leqq 360°$). In order to obey the zone of influence, more than one hundred x steps had to be taken to cover one foot of length. With this x step-size, the solution changed very little from plane to plane. Solutions with as few x stations as 10 points yielded results within 4% of the aforementioned solution, even though the zone of influence was violated grossly. This result probably is caused by the relatively weak infleunce of the linear increase in wall crossflow caused by spin.

The rather direct influence of the primary-flow wall shear on boundary-layer thickness can be seen by observing the variation in the three-dimensional displacement thickness (Δ) defined by Moore[17] (Fig. 5). (In regions of high shear, the displacement thickness is calculated by solving a partial differential equation involving δx and $\delta\phi$, defined by Moore[17] and the method is outlined in Part II of the investigation. As shown in Fig. 5, which is for the same conditions as those discussed previously, spin greatly distorts the symmetry of the boundary layer. Near the cone tip ($x = 0.1$ ft), where the spin velocity is low, the boundary-layer structure has not been altered very much; however, away from the tip ($x = 1$ ft), the location of maximum thickness has moved approximately 50° into the region of negative wall crossflow. This distortion of the boundary-layer thickness, of course, is responsible for the displacement-thickness contribution to the Magnus force. Another interesting feature of the displacement-thickness calculation can be seen by observing the dotted curve with the T_w/T_0 marking equal to 0.56. Since this temperature ratio is that of the wall to the stagnation temperature, it corresponds to a cold wall. As can be seen from Fig. 5, a cold wall considerably thins and smooths out the boundary-layer displacement thickness and thus decreases the Magnus force. This effect may possibly have an influence in controlling the Magnus force in a practical situation.

Investigations such as Ref. 14 on nonspinning cones have shown that the boundary-layer equations give results that agree with experiments for small angles of attack. At angles of attack that approach the cone half-angle, the boundary approximation breaks down near the leeward side of the cone, and the boundary region equations seem to give a better description. The same general situation also seems to hold for the spinning-cone case. For example, at approximately 6° angle of attack, the primary-flow wall shear approaches zero on the negative crossflow side at a spin rate of 30,000 rpm. When this occurs, all of the flow quantities change very rapidly, and the need for boundary region techniques becomes evident. Shown in Fig. 6 is the displacement thickness Δ for a 6° case, and it shows that Δ changes very rapidly near $\phi = -150°(210°)$. (The primary-flow wall shear actually changes at a more rapid rate.) Therefore, there is a definite need for boundary-region techniques at moderate and high angle of attack, but the boundary-layer approximation is valid and useful for the ballistically important case of small angle of attack.

A series of graphs now will be presented which will illustrate the relative magnitude and importance of the centrifugal pressure difference, primary-flow wall stress, and crossflow wall stress on the Magnus force for various values of flow parameters. Figure 7 shows the angular variation of

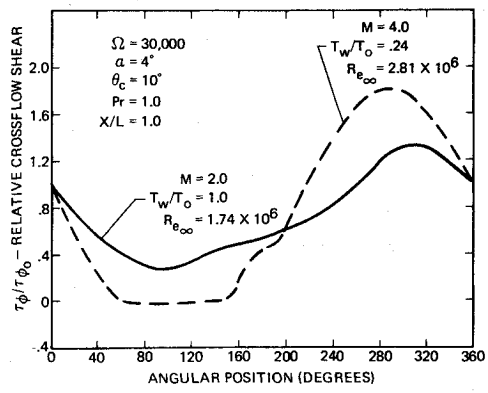

Fig. 8 Variation of crossflow wall shear.

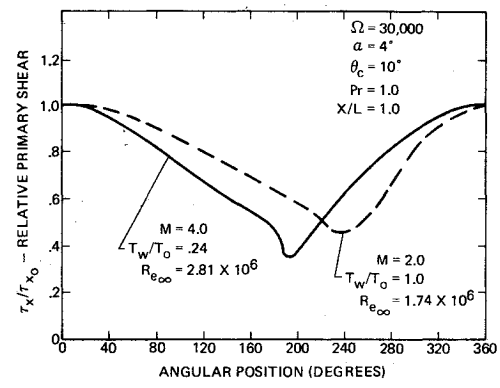

Fig. 9 Variation of primary-flow wall shear.

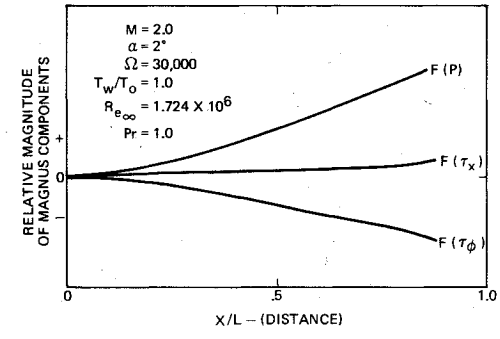

Fig. 10 Axial variation of Magnus components.

the pressure difference across the boundary layer due to crossflow. This pressure difference is calculated from the y-direction momentum, for example,

$$\Delta p = \cos\theta \int_0^\delta \frac{\rho w^2}{r}\, dy$$

and Δp has been normalized by its value on the windward inviscid symmetry line. The curves in Fig. 7 are for two different spin velocities, and it is seen that the pressure difference is positive and greater on the side of positive crossflow. The symmetry of the inviscid pressure around the cone implies that the cone body pressure will be less on the side of positive crossflow and a force generated perpendicular to the plane of angle of attack in the $-90°$ to $+90°$ direction. For a spin rate of 10,000 rpm, the centrifugal pressure difference varies greatly because of the fact that the spin and inviscid crossflow velocities have similar magnitudes. At 30,000 rpm, the spin crossflow velocity dominates and the pressure difference does not vary nearly as much. However, if the ratios of the pressure differences on opposite sides of the cone are compared, they have similar magnitudes.

In general it was found that the centrifugal pressure difference was the second largest of those generating the Magnus force, with the displacement thickness usually being the largest contributor. In all cases, however, the centrifugal pressure difference was of equal importance, compared with the displacement effect.

Another mechanism of importance was the contribution of the crossflow wall shear stress to the Magnus force. The force is calculated by multiplying the local crossflow wall shear stress by appropriate area and geometric factors for the cone, then integrating over the cone surface. Figure 8 illustrates the variation of the crossflow wall-shear stress around the cone for Mach numbers of both two and four. Again, the ordinate value has been normalized by the value at $\phi = 0°$, and the spin rate was 30,000 rpm. The Mach number four case is very interesting, since the wall-crossflow velocity has just the right value to cause the crossflow shear stress to go to zero over a significant portion of the positive crossflow side. This, of course, causes the stress to be very high on the opposite side of the cone, as seen in Figure 8. The overall effect of this situation is for the crossflow wall-stress contribution to the Magnus force to be large for this $M = 4$ case, and its value turned out to be almost equal and opposite to the centrifugal pressure difference force. For the Mach number two case the trends are similar, but the values of the spin and inviscid crossflow do not match as well, and the influence of crossflow wall stress is not quite as great.

Another minor contributor to the Magnus force is the difference in primary-flow wall stress from one side of the cone to the other. The behavior of this component with Mach number is just the opposite of the crossflow stress previously discussed, and is shown in Fig. 9. For the case of Mach number four, the primary-flow stress distribution is almost symmetrical, and the influence of spin is minor for a spin angular velocity of 30,000 rpm. When the Mach number had a value of two, spin caused a significant distortion of the primary-flow wall stress, and the infleunce of this Magnus force mechanism was larger, but still small compared with the other mechanisms.

The relative magnitude of the actual integrated forces for these three components is shown in Fig. 10 as a function of distance along the cone surface. The largest force contributor was the centrifugal pressure difference [marked $F(P)$], and the smallest was the primary-flow wall shear, which was approximately 11% of the centrifugal force. The crossflow wall stress is opposite in direction to the other two and was approximately 60% of the centrifugal pressure-difference force. All of the forces seem to grow with a slight nonlinearity with-x, and they are in an almost constant ratio from the cone tip to rear. For the flow situation given in Fig. 10, the displacement-thickness contribution was approximately 70% greater than the centrifugal pressure-difference force, and was in the same direction.

The actual values of the Magnus coefficients will not be given in Part I of the paper, since it is more appropriate to present the complete values with the displacement effect included. Therefore, the total value of the Magnus coefficients will be given in Part II, where the displacement-thickness contribution is given in detail.

In order to illustrate the influence of flow-parameter variation on the boundary-layer forces contributing to the Magnus effect, a wide variation of the parameters was studied. The following variations were carried out:

$$1.5 \leqq M \leqq 4.0 \qquad 0.24 < T_w/T_0 < 1.0$$

$$0 \leqq \Omega \leqq 30{,}000 \qquad 0 < \alpha \leqq 6°$$

Not all of the flows were varied over the entire range shown, but the previous listing represents the total parameter range covered. Some of the results are shown in Figs. 11 and 12,

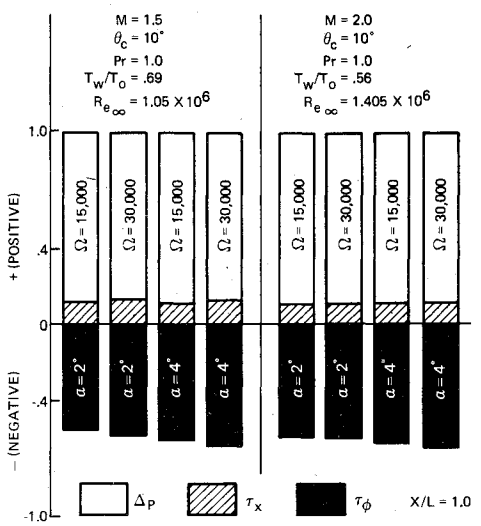

Fig. 11 Magnitude of Magnus forces.

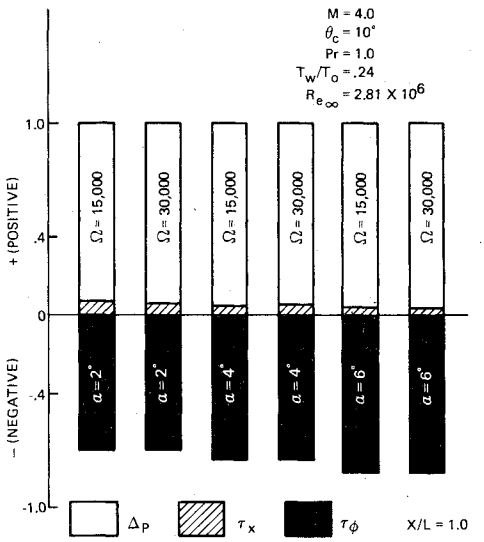

Fig. 12 Magnitude of Magnus forces.

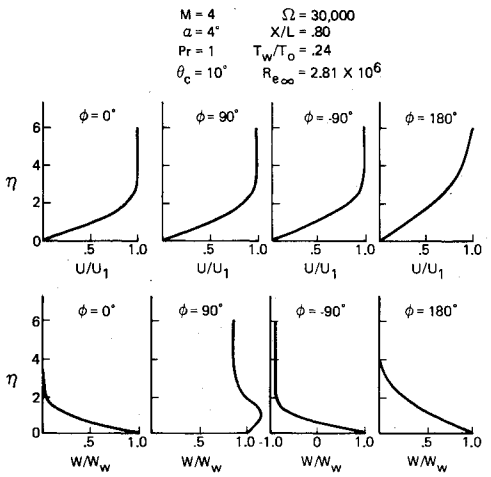

Fig. 13 Velocity profiles.

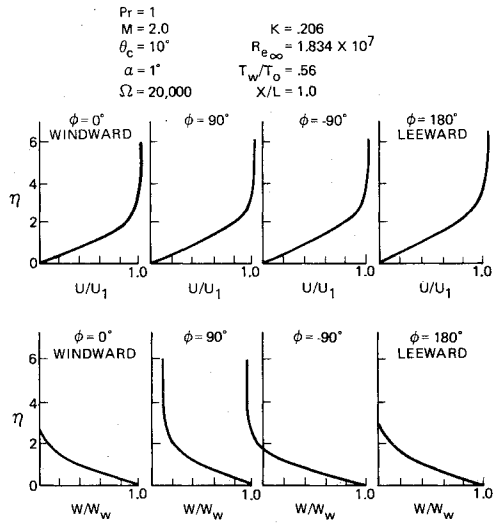

Fig. 14 Velocity profiles.

where the relative variations in the integrated forces are presented for a cone one foot long with a ten-degree-half-angle cone. Figure 11 exhibits Magnus force components for the two Mach numbers of 1.5 and 2.0 with a cold wall. The angle of attack for both Mach numbers was only taken to 4°, since the flows showed a marked tendency toward "separation" between the 4° and 6° angle of attack (there is no difficulty with the nonspinning solutions, and the rapid decrease in the primary-flow wall shear on the leeward side was due to spin near the rear of the cone). In order to treat the problem at higher angle of attack, a boundary-region technique is needed. The relative magnitudes of the Magnus components are seen to remain remarkably fixed with spin, angular velocity, Mach number, and angle of attack, as shown by Fig. 11. The contribution of the primary-flow wall stress (τ_x) was between 10 and 12% of the centrifugal pressure difference force (Δp), whereas the crossflow wall stress (τ_ϕ) was between 45 and 55% of the same force, but with opposite sign.

A somewhat different result was obtained for the case of Mach number four, as shown in Fig. 12. The crossflow wall stress contribution to the Magnus force varied between 70 and 80% of the centrifugal pressure difference force and was again in the opposite direction. The primary wall stress contribution was reduced to values between 4 and 8%, thus indicating very little distortion of the primary-flow wall stress angular distribution. Again, the angle of attack and spin rate had a minimal effect on the ratio of the force components. The change in the relative magnitude of the forces from the lower Mach number cases was due to the matching of the spin and inviscid crossflow velocities. For the Mach four case, the crossflow wall stress is low on one side of the cone and high on the other, and this can be easily seen from the velocity profiles shown in Fig. 13. At $\phi = 90°$, the crossflow velocity gradient is relatively low compared with the $\phi = -90°$, and this condition is the result of the wall crossflow velocity being almost equal in value to the inviscid crossflow velocity. It should also be noticed in Fig. 13 that the primary-flow velocity gradient changes by only a small amount with ϕ, but the Magnus force is a very small force. The main reason that the primary-flow wall stress force is small is that it is proportional to the $\sin\theta_c$, which has a small value for $\theta_c = 10°$. A typical set of velocity profiles for the lower Mach number conditions is shown in Fig. 14. For these conditions, the wall crossflow velocity caused by spin dominates the inviscid crossflow, and the wall crossflow stress remains relatively uniform around the entire cone. Therefore, it can be concluded that a sort of resonance condition exists when the spin and inviscid crossflow velocities have similar values.

It should be mentioned again that the actual values of the Magnus force and of the coefficients for these three force components are given in Part II of the paper, along with the displacement thickness contribution to the Magnus force. The reason that this format was chosen was that the displacement thickness force requires a different and difficult method of

calculation. Therefore, the first part of the paper serves to illustrate the structure of the boundary-layer flow and how it responds to parameter variations.

Computation Time

The boundary-layer calculations that have just been presented required five minutes of computation time on a CDC 6600 for the solutions obeying the zone of influence (100 × steps). Therefore, computer time will not be a limiting factor in extending the method to nonconical bodies, and turbulent flow if one has a very large machine like a CDC 7600.

Conclusions

For a complicated paper like the present one, it is worthwhile to present the conclusions in numbered order, so that they can be summarized concisely. The major conclusions that can be drawn from this research are the following:

1. A numerical method based on the physics of the boundary-layer approximation has been used to solve the laminar boundary-layer flow accurately over a spinning right circular cone at angle of attack in supersonic flow. Since the spinning cone problem is one of the more difficult three-dimensional boundary-layer problems, it is expected that this method will be useful when applied to other problems.

2. A comparison of the numerical solution with a series solution developed by Sedney showed that there was general qualitative agreement. However, the series solution is limited in accuracy because of the limited number of terms that have been calculated.

3. For the ballistically important case of small angle of attack, the boundary-layer approximation is a very accurate description of flow over a spinning cone at angle of attack. Boundary-region equations are not needed until the angle of attack acquires moderate values.

4. There are four significant forces that have been identified as being due to the spin-boundary-layer interaction. These forces, in order of their usual importance, are due to: a) displacement thickness, b) centrifugal pressure differences, c) crossflow wall shear stresses, and d) primary-flow wall shear stresses. Only the primary-flow shear stress has a value significantly smaller than that of the other forces in a typical flow situation.

5. The relative importance of the four Magnus force components depends to a large extent on the flow conditions. In particular, the crossflow shear component discussed in Part I will increase in value when the wall crossflow velocity and inviscid flow velocity have similar magnitudes. This effect can lead to a substantial cancelling of the Magnus force components. It is possible that other unusual conditions can arise, and these must be found with future calculations.

References

[1] Sedney, R., "Laminar Boundary Layer on a Spinning Cone at Small Angles of Attack in a Supersonic Flow," *Journal of Aerospace Sciences,* Vol. 24, June 1957.

[2] Vaughn, H. R. and Reis, G. E., "A Magnus Theory," AIAA Paper 73-124, Washington D.C., 1973.

[3] Lin, T. C. and Rubin, S. G., "Viscous Flow over Spinning Cones at Angle of Attack," *AIAA Journal* Vol, 12, July 1974, pp. 965-974.

[4] Sturek, W. B., "Boundary-Layer Studies on a Spinning Cone," AIAA Paper 72-967, Palo Alto, California, Sept. 1972.

[5] Sturek, W. B., "Boundary-Layer Studies on Spinning Bodies of Revolution, USA Ballistic Research Laboratories, Aberdeen Proving Ground, Maryland, BRL Rept. No. 2381, May 1974.

[6] Moore, F. K., "Laminar Boundary Layer on a Circular Cone in Supersonic Flow at Small Angle of Attack," NACA TN 2521, Oct. 1951.

[7] Jones, D. J., "Tables of Inviscid Supersonic Flow About Circular Cones at Incidence $\gamma = 1.4$," AGARDograph 137, 1969.

[8] Dwyer, H. A., "Solution of a Three-Dimensional Boundary Layer Flow with Separation," *AIAA Journal,* Vol. 6, July 1968, pp. 1336-1342.

[9] Dwyer, H. A., "Calculation of Unsteady and Three-Dimensional Boundary-Layer Flows," *AIAA Journal,* Vol. 11, June 1973, pp. 773-774.

[10] Wang, K. C., "Laminar Boundary Layer Over a Body of Revolution at Extreme High Incidence," *Physics of Fluids,* Vol. 17, July 1974, pp. 1381-1385.

[11] Kraus, E., "Comment on Solution of a Three-Dimensional Boundary Layer Flow with Separation," *AIAA Journal,* Vol. 7, March 1969, p. 575.

[12] Blottner, F. G., "Three-Dimensional, Incompressible Boundary Layer on Blunt Bodies," Sandia Laboratories, Albuquerque, Rept. SLA-73-0366, April 1973.

[13] Wang, K. J., "On the Determination of the Zones of Influence and Depence for Three-Dimensional Boundary Layer Equations," *Journal of Fluid Mechanics,* 43,1, 1973.

[14] Dwyer, H. A. and Sanders, B. R., "A Physically Optimum Difference Scheme for Three-Dimensional Boundary Layers," 4th International Conference on Numerical Methods in Fluid Dynamics, Boulder, Colorado, June 24-28, 1974; Springer-Verlag, *Lecture Notes in Physics.*

[15] Dwyer, H.A., "Boundary Layer on a Hypersonic Sharp Cone at Small Angle of Attack," *AIAA Journal,* Vol. 9, Feb. 1971, pp. 277-284.

[16] Dwyer, H.A. and McCroskey, W.J., "Crossflow and Unsteady Boundary Layer Effects on Rotating Blades," *AIAA Journal,* Vol. 9, Aug. 1971, pp. 1498-1505.

[17] Moore, F.K., "Displacement Effects of a Three-Dimensional Boundary Layer," NACA, TN 2722, June 1972.